Polymer Journal Vol. 4, No. 2, pp 172—182 (1973)

Structural Studies of Polyformals, $[—OCH_2O—(CH_2)_m—]_n$. I. Poly(1,3-dioxepane)

Shintaro SASAKI, Yasuhiro TAKAHASHI, and Hiroyuki TADOKORO

Department of Polymer Science, Faculty of Science, Osaka University, Toyonaka, Osaka 560, Japan.

(Received March 13, 1972)

ABSTRACT: The crystal and molecular structure of poly(1,3-dioxepane) $[—OCH_2O—(CH_2)_4—]_n$ has been determined by X-ray diffraction and infrared spectroscopic methods. The cell constants are a=8.50 Å, b=4.79 Å, and c(fiber axis)=13.50 Å, and the space group is P2cn(C_{2v}^9). Two molecular chains pass through a unit cell. A molecular chain contains two monomeric units in the fiber identity period, and has a structure of the glide type which deviates slightly from the $TG\bar{T}G_2T\bar{G}TGT\bar{G}_2$ conformation,

$$(—CH_2—CH_2—CH_2—CH_2—O—CH_2—O—CH_2—CH_2—CH_2—CH_2—O—CH_2—O—)_n$$
$$T\quad G\quad T\quad \bar{G}\quad T\ G\quad G\ T\quad \bar{G}\quad T\quad G\quad T\ \bar{G}\quad \bar{G}$$

where T, G, and $\bar{G}$ denote the *trans* and two types of *gauche* forms, respectively. The COCOC sequences take the *gauche—gauche* forms in a way similar to poly(oxymethylene). From the present result, it was confirmed that bond scission of the 1,3-dioxepane ring occurs exclusively at the same type of bond, giving rise to the regular head-to-tail polymer in cationic polymerization.

KEY WORDS Structure of Poly(1,3-dioxepane) / X-ray Diffraction / Normal Coordinate Treatment / Constrained Least-Squares Method / Dipole Interaction / Bond Scission /

In previous papers, structural studies of the series of polyethers $[—(CH_2)_m—O—]_n$ have been reported.[1-5] There is another series of polyethers expressed by the general formula $[—OCH_2O—(CH_2)_m—]_n$, namely polyformals. The first member (m=1) polyoxymethylene (POM), which is also the first member of the $[—(CH_2)_m—O—]_n$ series, has a high melting point (180°C) and is insoluble in ordinary solvents at room temperature, but the second member (m=2) poly(1,3-dioxolane) has a low melting point (55°C) and easily soluble in water at room temperature, resembling poly(ethylene oxide). The fourth member (m=4) poly(1,3-dioxepane) has a lower melting point (24°C) and is insoluble in water. It is of considerable interest to relate these differences in properties with their structures.

In cationic ring-opening polymerization of cyclic formals, the question arises whether the bond scission occurs exclusively at the same type of bond, for example bond I, or at both bonds I and II at random. If the scission

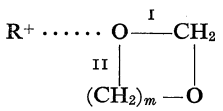

occurs at random, the resultant polymer should generally not have a well-defined crystal structure. However, there are several polymers that give highly crystalline X-ray patterns despite the irregular sequences. The best known example is atactic poly(vinyl alcohol).[6] Poly(methylene polysulfides) $(—CH_2—S_x—)_n$ with nonstoichiometric values of x=1.5—3.0 also give very sharp X-ray fiber diagrams.[7] Accordingly, one must be very careful not to conclude that a polymer has a regular structure from a sharp X-ray diffraction pattern alone. In the case of polyformals, the regular structure results from the regular bond scission. The structure analysis will serve to make clear the mechanism of the polymerization.

Polyformals are the alternating copolymers of formaldehyde and ω-glycols. In these polymers, the COC dipole moments are closely

adjacent to each other at the COCOC sequences in the similar fashion to POM. It may be of considerable interest to discuss the conformation of the COCOC part in comparison with that of POM.

Polymerization of cyclic formals has been investigated by Hill and Carothers,[8] Yamashita, *et al.*,[9,10] and others.[11] But the structures of the series of polyformals have apparently not yet been published to date except for POM. Structural studies of this series are now in progress in this laboratory. Three crystalline modifications of poly(1,3-dioxolane) were found, and termed as modifications I, II, and III. The crystal structure of modification II was recently determined, and will be published shortly.[12] Oleinik and Yenikolopyan reported the infrared spectra of poly(1,3-dioxolane), but they did not refer to the modifications.[13]

In advance of poly(1,3-dioxolane), the structure of the fourth member poly(1,3-dioxepane) was determined, and is reported in the present paper. This work was carried out by a combination of X-ray diffraction and infrared spectroscopic studies. Factor group analyses gave the information about the symmetry of a molecular chain, and the normal coordinate treatment of skeletal models served for the determination of the molecular model. In the final refinement of the crystal structure, the constrained least-squares method by internal coordinates was of great value.[14,15]

EXPERIMENTAL

Sample

1,3-Dioxepane of commercial source was polymerized in sealed glass tubes with $AlEt_2Cl$ catalyst at 0°C for about five days. The polymer was washed with aqueous NH_3 solution, extracted with benzene, and purified by reprecipitation from an acetone solution with methanol. The polymer was waxy and the melting point measured by using a polarizing microscope is 24°C. The density measured at 0°C by the flotation method by using aqueous solution of calcium chloride was 1.14 g/cc.

X-ray Diffraction

X-ray diffraction measurements were carried out by using Ni-filtered CuKα radiation. The uniaxially oriented fiber specimen was prepared according to the following procedure. The molten sample was drawn to a fiber of diameter of about 0.5 mm by using two tweezers in Dry Ice—methanol mixture, and then crystallized by standing on Dry Ice for about one hour. During the X-ray measurements the fiber specimen was cooled with a cold air-stream passed through a Dry Ice—acetone trap in order to prevent deformation and fusion of the sample. An X-ray fiber photograph is shown in Figure 1. A Weissenberg photograph was taken by setting the uniaxially oriented fiber specimen with the fiber axis perpendicular to the camera axis and oscillating the specimen through 180° about the camera axis. The photograph is given in Figure 2 with its schematic representation. The number of the independent observed reflections was 37.

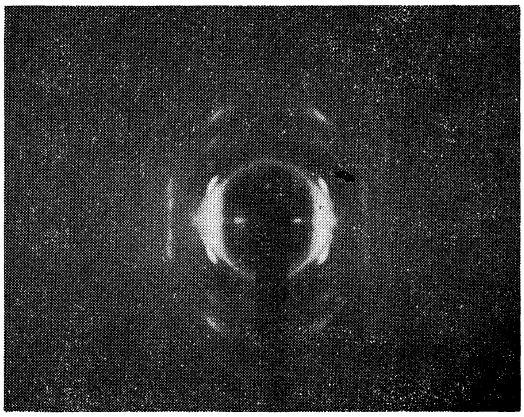

Figure 1. X-ray fiber photograph of poly(1,3-dioxepane).

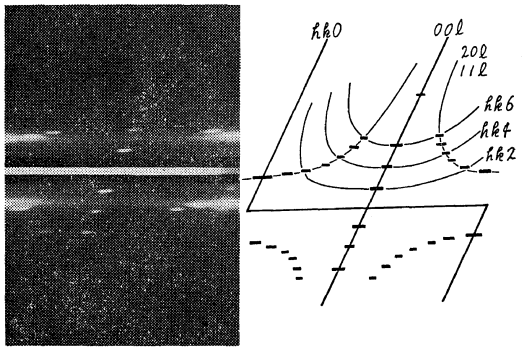

Figure 2. Weissenberg photograph and its schematic representation of poly(1,3-dioxepane).

The reflection intensities obtained by a multiple film method were measured visually by using a standard intensity scale.

Infrared Absorption Spectra

The oriented film specimen for the far-infrared measurement was obtained by rolling the molten sample at 0°C.

The sample for the measurement in the 4000—700 cm^{-1} region was prepared by rolling the film between two thin AgCl sheets at 0°C. The infrared measurements were made by using a low temperature cell. A Dry Ice—methanol mixture was used for the measurement in the 4000—500 cm^{-1} region with a Japan Spectroscopic Co. DS-402G grating infrared spectrophotometer, and liq. N_2 was also used in the 500—80 cm^{-1} region with a HITACHI Model FIS-1 double beam far-infrared spectrophotometer. The polarized spectra in the 1500—80 cm^{-1} region and the frequencies are given in Figure 3 and Table I.

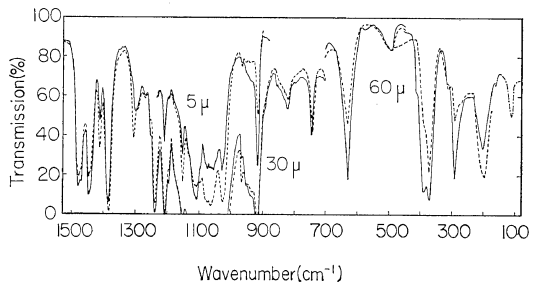

Figure 3. Polarized infrared spectra of poly(1,3-dioxepane). Electric vector to elongation: (——) perpendicular; (----) parallel; (—·—) non-polarized data.

ANALYSIS AND RESULT

Unit Cell

All the observed reflections were indexed with an orthorhombic unit cell of a=8.50 Å, b=4.79 Å, and c(fiber axis)=13.50 Å. The molecular chain contains two chemical units in the fiber identity period. This period is far shorter than the value calculated by assuming the planar zigzag conformation, 16.88 Å. The density (1.23 g/cc) calculated by assuming that two molecular chains pass through a unit cell, is reasonable in comparison with the observed value (1.14 g/cc).

Table I. The infrared spectra of poly(1,3-dioxepane)

Frequency, cm^{-1}	Dichroism	Intensity
2948	⊥	sh
2920	⊥	vs
2872	⊥	vs
2857	⊥	vs
1477	⊥	m
1476	//	m
1468	⊥	m
1443	⊥	m
1438	⊥	sh
1408	//	w
1380	⊥	s
1379	//	s
1303	//	w
1297	⊥	w
1266	⊥//	vvw
1250	⊥	sh
1237	⊥	s
1207	⊥//	s
1194	⊥	w
1151	//	vs
1114	⊥	sh
1106	⊥	vvs
1095	//	sh
1078	···	sh
1074	//	vvs
1063	//	vvs
1054	···	sh
1029	⊥	vs
1024	//	vvs
966	//	vvw
948	⊥	sh
936	⊥	sh
914	⊥	vs
822	⊥	w
819	//	w
743	⊥	w
741	//	w
630	⊥	m
495	···	vvw
410	⊥	sh
388	⊥	m
369	//	m
367	⊥	m
311	//	vvw
290	⊥	w
199	⊥	w
196	//	w
112	···	vw

The systematic absences $l \neq 2n$ for $00l$ were clear from the Weissenberg photograph, but the other systematic absences were not so obvious since there were only four $hk0$ reflections and many reflections overlapped owing to the axial ratio a/b being accidentally near to $\sqrt{3}$. It was difficult to determine whether the systematic absences were (a) $h+k \neq 2n$ for $hk0$, or (b) $h \neq 2n$ for $h00$ and $k \neq 2n$ for $0k0$. In addition, the possibility of the systematic absences $l \neq 2n$ for $h0l$ was also considered. Consequently, the possible space groups were $P2_1cn(C_{2v}^9)$ (the systematic absences $h+k \neq 2n$ for $hk0$ and $l \neq 2n$ for $h0l$), and $P2_12_12_1(D_2^4)$ ($h \neq 2n$ for $h00$, $k \neq 2n$ for $0k0$, and $l \neq 2n$ for $00l$). These two space groups have four equivalent general positions. Since four chemical units are contained in a unit cell, the molecular chain must have the symmetry which coincides with one of the symmetry elements of the crystal lattice. The space group $P2_1cn(C_{2v}^9)$ requires that the molecular chain has the glide plane, while $P2_12_12_1(D_2^4)$ requires the twofold screw axis. Discrimination between these two cases is possible from the infrared study as is discussed below.

Molecular Models

As discussed above, the molecular symmetry should be isomorphous to the point group C_s or C_2. The results of the factor group analyses are shown in Tables II a and II b.

Table II. Factor group analyses and selection rules of poly(1,3-dioxepane) isolated single chain under the factor group (a) C_s and (b) C_2

(a) Molecular group C_s

C_s	E	$\sigma_g(zx)$	N[a]	IR[b]
A′	1	1	$51-T_x, T_z$	a(⊥, //)
A″	1	−1	$51-T_y, R_z$	a(⊥)

(b) Molecular group C_2

C_2	E	C_2^s	N[a]	IR[b]
A	1	1	$51-T_z, R_z$	a(//)
B	1	−1	$51-T_x, T_y$	a(⊥)

[a] N, number of total modes; T, R, translation and rotation of a molecule as a whole.
[b] a, active; f, forbidden.

Table III. Factor group analyses and selection rules of poly(1,3-dioxepane) isolated single chain under the factor group (a) C_{2h} with the glide plane and (b) C_{2h} with the twofold screw axis[a]

(a) Molecular group C_{2h} with the glide plane

C_{2h}	E	$C_2(y)$	i	$\sigma_g(zx)$	N	IR
A_g	1	1	1	1	25	f
B_g	1	−1	1	−1	$26-R_z$	f
A_u	1	1	−1	−1	$25-T_y$	a(⊥)
B_u	1	−1	−1	1	$26-T_x, T_z$	a(⊥, //)

(b) Molecular group C_{2h} with the twofold screw axis

C_{2h}	E	$C_2^s(z)$	i	$\sigma(xy)$	N	IR
A_g	1	1	1	1	$27-R_z$	f
B_g	1	−1	1	−1	24	f
A_u	1	1	−1	−1	$24-T_z$	a(//)
B_u	1	−1	−1	1	$27-T_x, T_y$	a(⊥)

[a] The notations are the same as in Table II.

Under the factor group C_s or C_2, 20 CH stretching modes, 10 CH_2 bending modes, 30 rotational modes of CH_2 groups (wagging, twisting, and rocking), 14 skeletal stretching modes, and 24 skeletal bending and torsional modes are infrared-active. Hewever the infrared spectra are rather simple as shown in Figure 3. The number of observed absorption bands is actually about one-half of these expected values. This fact suggests that the molecular symmetry should be higher than the C_s or C_2 approximately. Accordingly, the existence of the center of symmetry was assumed at this stage so that the molecular symmetry might be isomorphous to the point group C_{2h}. There are two possible cases of C_{2h} symmetry, which consist of (a) the glide plane (along the fiber axis) and the twofold axes perpendicular to this plane, and (b) the twofold screw axis (coinciding with the fiber axis) and the mirror planes perpendicular to this axis. The results of the factor group analyses are given in Tables III a and III b. In these cases, 10 CH stretching modes, 5 CH_2 bending modes, 15 rotational modes of CH_2 groups, 6 skeletal stretching modes, and 12 skeletal bending and torsional modes are infrared-active. The A_u species for the case (b)

Table IV. The correlations of the molecular, site and space groups of the C_{2h} molecular symmetries (a) with the glide plane and (b) with the twofold screw axis[a]

(a) The case with the glide plane

Molecular group (C_{2h})		Site group (C_s)		Space group (C_{2v}^9)	
A_g	f			A_1	a(⊥)
B_g	f	A′	a(⊥, //)	A_2	f
A_u	a(⊥)	A″	a(⊥)	B_1	a(//)
B_u	a(⊥, //)			B_2	a(⊥)

(b) The case with the twofold screw axis

Molecular group (C_{2h})		Site group (C_2)		Space group (D_2^4)	
A_g	f			A	f
B_g	f	A	a(//)	B_1	a(//)
A_u	a(//)	B	a(⊥)	B_2	a(⊥)
B_u	a(⊥)			B_3	a(⊥)

[a] The notations are the same as in Table II.

should have parallel dichroism, and the B_u species perpendicular dichroism. On the other hand, the A_u species for the case (a) have perpendicular dichroism, but the B_u species have transition moments not having definite directions, but parallel to the glide plane. Tables IV a and IV b show the symmetry species and infrared selection rules for the molecular, site, and space groups of these two cases. The correlations between the symmetry species are also given. The B_u modes of the molecular group of the case (a) (glide type) will be split into the perpendicular (A_1) and the parallel bands (B_1) due to the intermolecular interaction between the two molecules in a Bravais lattice. On the other hand, case (b) will lead to the splitting of the perpendicular B_u modes into two perpendicular bands (B_2 and B_3). In the spectra, the bands at about 1477, 1380, 820, 742, 368, and 198 cm^{-1} exhibit splitting into the parallel and perpendicular bands. This fact suggests case (a), that is, the C_{2h} molecular symmetry with the glide plane and the space group $P2_1cn(C_{2v}^9)$.

If the systematic absences $k \neq 2n$ for $0kl$ were added to those of the space group $P2_1cn(C_{2v}^9)$, the space group would become $Pbcn(D_{2h}^{14})$, in which the C_{2h} molecular symmetry with the glide plane is reguired. However weak reflections with the indices 014, 015, and 016 could be observed. This fact suggests that the structure deviates slightly from the space group $Pbcn(D_{2h}^{14})$. After the final refinement of the crystal structure, it was found that the molecular symmetry is not exactly the C_{2h} type, but at this stage molecular models were assumed to have the exact C_{2h} symmetry with the glide plane for convenience of consideration. The numbering of the atoms are as follows.

$$-O(7')-\Big|-C(1)-O(2)-C(3)-C(4)\overset{i}{-}C(5)-C(6)-O(7)-\Big|-C(1'')-$$

	A	*T*	*B*	*T*	$\bar{B}$	*T*	$\bar{A}$	
I	*G*	*T*	$\bar{G}$	*T*	*G*	*T*	$\bar{G}$	$\bar{G}TGT\bar{G}TG$
II	*G*	*T*	*T*	*T*	*T*	*T*	$\bar{G}$	$\bar{G}T_5G$
III	*T*	*T*	*G*	*T*	$\bar{G}$	*T*	*T*	$T_2\bar{G}TGT_2$

The center of symmetry must be at the midpoint of the C(4)—C(5) bond from the chemical structure of this polymer. Therefore, this bond must have the *trans* form. The O(2)—C(3) and C(6)—O(7) bonds of CCOC type could not take the *gauche* form, because of the inadequate spacing between the attached two CH_2 groups from the consideration of the van der Waals radius of CH_2 group, as discussed in the structures of other polyethers such as poly(ethylene oxide)[16,17] and polyoxacyclobutane.[3] Thus, these bonds would take the *trans* form. The other bonds can take either of the *trans* or the *gauche* forms. The conformations of the C(1)—O(2) and the O(7)—C(1″) bonds, *A* and $\bar{A}$, are the right- and left-handed forms, since the center of symmetry is located at the midpoint of the C(4)—C(5) bond. The conformations of the C(3)—C(4) and the C(5)—C(6) bonds, *B* and $\bar{B}$, are also in the same relation.

Under these assumptions, ideal molecular models of the C_{2h} symmetry of the glide type

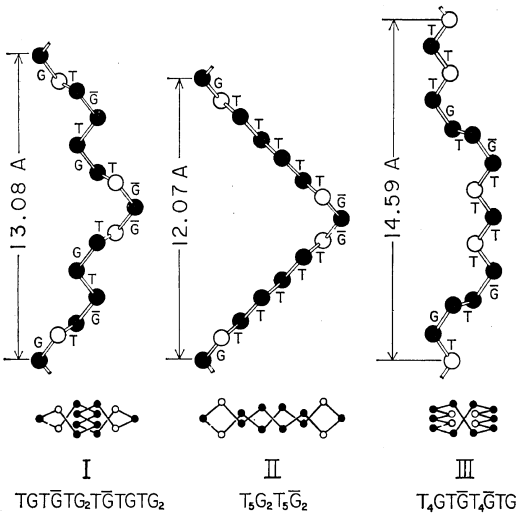

Figure 4. Possible molecular models of poly(1,3-dioxepane).

were considered. The combination of the *trans* and the *gauche* forms in *A* and *B* gives five cases as follows; (*T*, *T*), (*T*, *G*), (*G*, *T*), (*G*, *G*), and (*G*, $\bar{G}$). The conformation of a chemical unit in the molecular chain is related with the next one by the glide plane. The cases (*T*, *T*) and (*G*, *G*) give fiber periods quite different from the observed value 13.50 Å. (*G*, $\bar{G}$), (*G*, *T*), and (*T*, *G*) give the possible models I, II, and III, respectively, each of which has a fiber period close to the observed value as shown in Figure 4.

Structure Factor Calculations

The glide plane of the molecular chain must coincide with the *c* glide plane of the space group. Although the positions of the two molecules in the *c* projection differ by (*a*/2, *b*/2) respectively, the position of the two molecules as a whole can be arbitrarily chosen along the *a* axis. Here, the centers of symmetry of the two molecules were placed tentatively at (1/4, 1/4) and (3/4, 3/4). Therefore, the position along the *c* axis remained to be determined. Structure factors of the models I, II, and III in the space group $P2_1cn(C_{2v}^9)$ were calculated by trial and error repetition method. At first, model III was excluded because of poor agreement between the observed and calculated intensities (I_o and I_c). From the result of the subsequent trial and error repetition for models I and II, model I was found to be more reasonable. The discrepancy factor $R(=\sum|\sqrt{I_o}-\sqrt{I_c}|/\sum\sqrt{I_o})$ for the 37 independent observed reflections was 0.24, when the fractional coordinate *z*[C(1)]=0.257, and the isotropic thermal factor $B=5.0$ Å^2 was used for all atoms. If *z*[C(1)]=0.250, the crystal structure would be $Pbcn(D_{2h}^{14})$. For model II distorted so as to give the observed fiber period 13.50 Å, the *R* factor could be only reduced to 0.38. The numerical computations were carried out by using the NEAC-2200 Model 500 electronic digital computer (Nippon Electric Co., Ltd.) installed in the Computation Center of this university. Model I was also supported by the calculations of the skeletal normal vibrations of the models.

Calculations of the Skeletal Normal Vibrations

The skeletal normal vibrations for the isolated single chains of the models I, II, and III were calculated according to Wilson's GF-matrix method by using the Urey-Bradley force field. The force constants are given in Table V. Here *K*(CC), *K*(CO), *H*(COC), $F_\tau(CO_T)$, F_τ(CC), and *F*(CO) were transferred from the values of poly(ethylene oxide) skeletal model,[18] and *H*(OCO), $F_\tau(CO_G)$, and *F*(OO) from POM.[19] For *H*(CCC), 0.30 was assumed by referring polyoxacyclobutane.[5] As discussed earlier, the

Table V. Force constants of poly(1,3-dioxepane)[a]

K(CC)	4.0 md/Å
K(CO)	4.5
H(COC)	0.45
H(OCO)	0.46
H(OCC)	0.30
H(CCC)	0.30
$F_\tau(CO_T)$	0.0454
$F_\tau(CO_G)$	0.061
F_τ(CC)	0.0495
F(CC)	0.40
F(CO)	0.44
F(OO)	0.62
F'	$-0.1F$

[a] The force constants, *K*, *H*, F_τ, and *F* indicate the stretching, bending, torsional, and repulsive force constants, respectively. CO_T and CO_G denote the CO bonds of the *trans* and *gauche* forms, respectively.

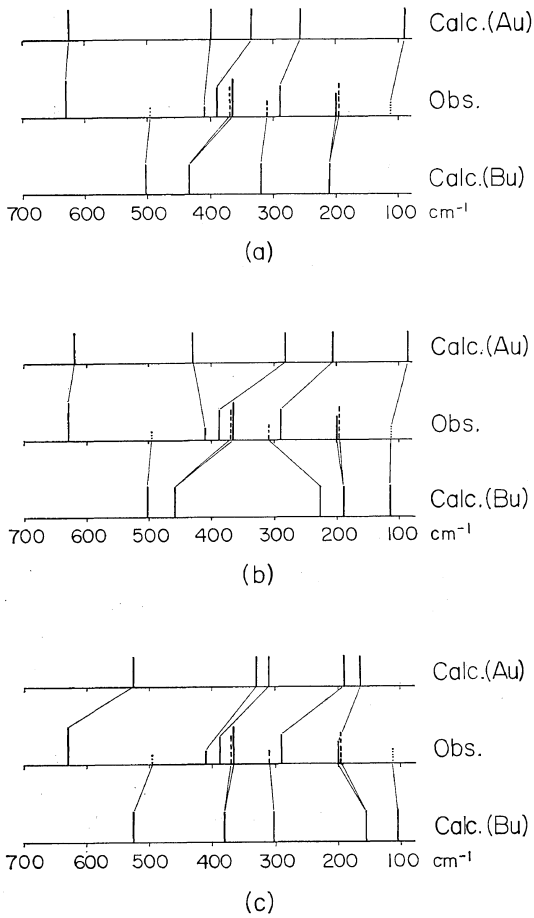

Figure 5. Comparison between the observed and calculated normal frequencies of poly(1,3-dioxepane) skeletal models (a) I, (b) II, and (c) III.

doublets at about 368 and 198 cm^{-1} should be assigned to the B_u species of the molecular group. The weak parallel band at 311 cm^{-1} may be assigned to the B_u species, although splitting was not observed, probably because of the weak intensity. The infrared-inactive A_g and B_g modes of the molecular group were considered to be infrared-active in the space group C_{2v}. However, these modes were not observed, probably due also to the weak intensity. The tentative assignments were carried out for the models I, II, and III. As Figure 5 shows schematically, the calculated frequencies for model I gave far better agreement with the observed ones in the far-infrared region, in comparison with those for the other models. The observed and the calculated frequencies for model I and the tentative assignments are given in Table VI.

Refinement of the Crystal Structure

The crystal structure deviates slightly from the space group Pbcn(D_{2h}^{14}). This space group requires the exact C_{2h} molecular symmetry with the glide plane, but the present structure $P2_1cn(C_{2v}^9)$ requires the C_s symmetry, that, is, only the glide plane of symmetry. The way in which the molecular chain is distorted from the model I of the C_{2h} symmetry is of considerable interest. The reflection intensity data were, however, rather poor, while 23 parameters must be determined, that is, the *xyz* coordinates of the seven skeletal atoms, overall thermal

Table VI. Skeletal vibrations of poly(1,3-dioxepane)

Species	Obsd frequencies (dichroism), cm^{-1}	Calcd frequencies (Model I), cm^{-1}	Assignment[a] (Potential energy distribution, %)
A_u	630 (⊥) m	620	δ(OCO)(46)+δ(COC)(28)
	410 (⊥) sh	398	δ(OCC)(43)−δ(CCC)(36)
	388 (⊥) m	336	δ(CCC)(38)−τ(OCCC)(16)
	290 (⊥) w	257	δ(COC)(50)−δ(OCO)(16)
	112 (···) vw	91	τ(COCO)(39)−τ(OCCC)(37)
B_u	495 (···) vvw	502	δ(COC)(63)
	369 (//) m 367 (⊥) m	433	δ(OCC)(54)−δ(CCC)(28)
	311 (//) vvw	320	δ(CCC)(44)+δ(OCC)(19)
	199 (⊥) w 196 (//) w	211	τ(COCO)(55)

[a] δ, Bending; τ, Torsion. The potential energy distribution less than 15% is neglected. The signs denote the phase relations of the coupled coordinates.

Table VII. Atomic coordinates of poly(1,3-dioxepane)[a]

Atom	x/a	y/b	z/c
C(1)	0.250	−0.133	0.254
O(2)	0.302	−0.005	0.344
C(3)	0.177	0.161	0.384
C(4)	0.240	0.327	0.472
C(5)	0.298	0.129	0.553
C(6)	0.348	0.310	0.641
O(7)	0.208	0.420	0.685

[a] The thermal factor B is 5.8 Å^2 for all atoms.

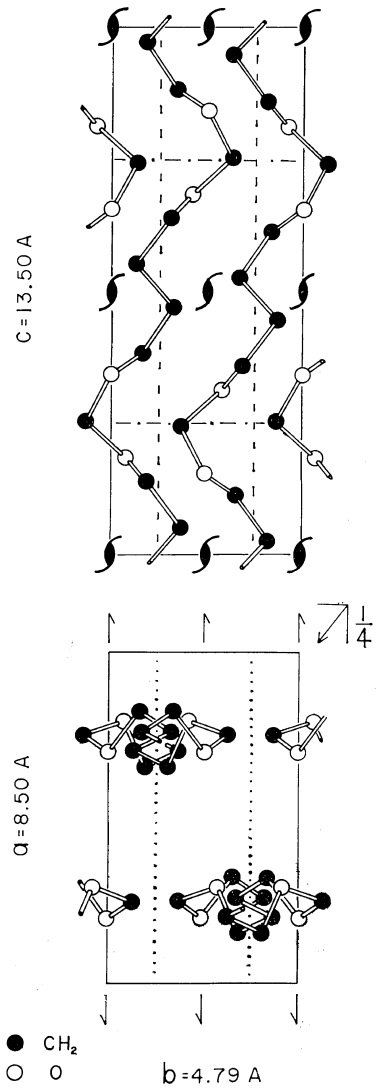

Figure 6. Crystal structure of poly(1,3-dioxepane).

Table VIII. Bond lengths, bond angles, and internal rotation angles

Bond lengths	
C—C	1.53 Å
C—O	1.43
Bond angles	
C(1)—O(2)—C(3)	109°
O(2)—C(3)—C(4)	109
C(3)—C(4)—C(5)	110
C(4)—C(5)—C(6)	107
C(5)—C(6)—O(7)	107
C(6)—O(7)—C(1″)	109
O(7)—C(1″)—O(2″)	109
Internal rotation angles	
O(7′)—C(1)—O(2)—C(3)	60°
C(1)—O(2)—C(3)—C(4)	187
O(2)—C(3)—C(4)—C(5)	−61
C(3)—C(4)—C(5)—C(6)	184
C(4)—C(5)—C(6)—O(7)	72
C(5)—C(6)—O(7)—C(1″)	192
C(6)—O(7)—C(1″)—O(2″)	−79

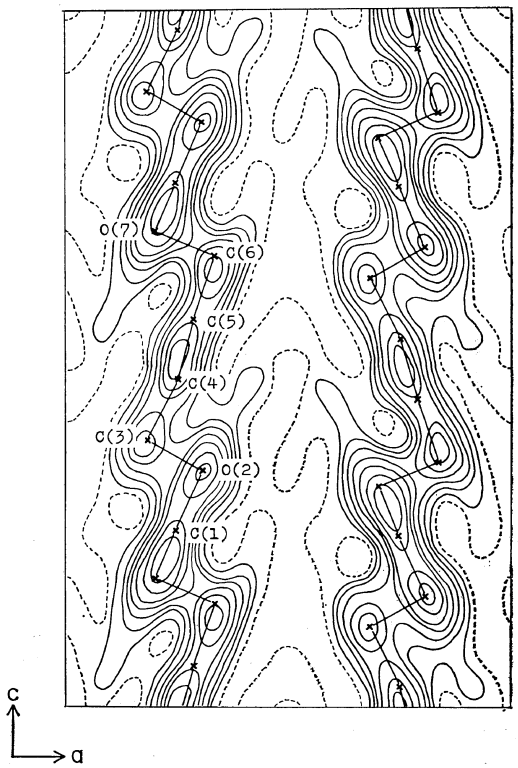

Figure 7. Electron density projection on the *ac* plane. Contours are at intervals of 1 e/Å^2. (----): 0 e/Å^2.

Table IX. Comparison between the observed and calculated intensities

h k l	$\sqrt{I_o}$ [a]	$\sqrt{I_c}$ [b]	h k l	$\sqrt{I_o}$ [a]	$\sqrt{I_c}$ [b]
2 0 0	207.0	190.1	4 0 4	50.0	28.0
1 1 0			2 2 4		
3 1 0	27.0	23.4	4 1 4	—	17.5
0 2 0			3 2 4	—	18.1
4 0 0	34.0	35.5	5 0 4	26.7	27.1
2 2 0			0 3 4		
5 1 0			5 1 4	23.3	20.6
4 2 0	16.0	24.0	4 2 4		
1 3 0			1 3 4		
0 1 1	—	17.7	2 3 4	—	11.6
1 1 1	94.5	111.0	6 0 4		
2 1 1	—	23.5	3 3 4	38.3	22.1
3 1 1	37.3	46.0	5 2 4		
0 2 1			0 1 5	31.2	23.8
1 0 2	—	15.4	1 1 5	62.3	60.8
0 1 2	—	19.5	2 1 5	34.8	32.4
2 0 2	70.6	54.8	3 1 5		
1 1 2			0 2 5	56.8	60.0
2 1 2	21.3	43.6	1 2 5		
3 0 2	—	11.3	2 2 5	31.2	39.4
3 1 2			1 0 6	16.0	23.1
0 2 2	45.3	49.5	0 1 6	12.0	6.2
1 2 2			2 0 6	28.0	32.1
4 0 2	28.0	25.3	1 1 6		
2 2 2			2 1 6	—	18.1
0 1 3	—	6.2	3 0 6	18.0	13.8
1 1 3	31.5	30.8	3 1 6		
2 1 3	21.0	19.6	0 2 6	28.0	28.0
3 1 3			1 2 6		
0 2 3	30.0	34.3	0 0 2	15.8	17.6
1 2 3			0 0 4	15.8	16.3
1 0 4	16.7	22.8	0 0 6	21.3	20.1
0 1 4	23.3	23.2	0 0 8	—	1.5
2 0 4	46.7	35.2	0 0 10	9.9	11.3
1 1 4			0 0 12	—	0.2
2 1 4	—	24.3	0 0 14	5.6	3.0
3 0 4	26.7	37.3			
3 1 4					
0 2 4	26.7	18.4			
1 2 4					

[a] The observed structure factors $\sqrt{I_o}$'s were put on the same scale as the $\sqrt{I_c}$'s by setting $\sum k\sqrt{I_o} = \sum \sqrt{mF_c^2}$, where k is the scale factor and m is the multiplicity.

[b] $\sqrt{I_c}$'s of the reflections which overlap on X-ray fiber photograph are $\sqrt{\sum mF_c^2}$.

factor, and the scale factor. At first, the refinement by the diagonal least-squares method was carried out. Although the discrepancy factor R was reduced from 0.24 to 0.13 after ten cycles of the least-squares repetition, the result was not acceptable since the bond lengths and bond angles deviate considerably from the standard values.

The full-matrix constained least-squares method was then applied to the refinement.[14,15] By fixing the values of the bond lengths and bond angles at the standard values, the number of

the variables could be reduced to 11, that is, the *yz* coordinates of the origin atom C(1), three Eulerian angles representing the molecular orientation, four torsional angles, the overall thermal factor, and the scale factor. The *x* coordinate of the origin atom can be arbitrarily chosen, and here $x[C(1)]=0.250$ was used. The result after ten cycles gave rather short interchain atomic distances (the shortest C ··· C distance: 3.47 Å), and the atomic coordinates were therefore slightly modified and the result is as shown in Table VII. The closest intermolecular contact is 3.61 Å for C ··· C. The discrepancy factor, 0.18, did not change with this procedure. The bond lengths, bond angles, and internal rotation angles calculated from the final atomic coordinates are listed in Table VIII. The crystal structure is shown in Figure 6 with its symmetry elements. Figure 7 shows the electron density map projected on the *ac* plane. The comparison between the observed and calculated intensities is given in Table IX.

DISCUSSION

The crystal structure deviates slightly from the space group Pbcn(D_{2h}^{14}). Figure 8 shows that the final molecular structure (b) is complicatedly deformed from the initial model (a). The values of the torsional angles considerably deviate from the exact *trans* (180°) and *gauche* angles (60° and −60°). As the result, the part of the upper half of the initial model shifts a little to the left as a whole, and the lower half to the right as shown in Figure 8.

Exactly speaking, the center of symmetry is not present, but the infrared spectra, especially the far-infrared spectra, could be approximately interpreted with the initial model under the factor group C_{2h}, probably because of the rather small deviation from the exact C_{2h} model.

In the case of POM, it was suggested that one of the important factors producing the helical structure is the intramolecular interaction of COC dipole mements.[20] This problem is also considered to be important in the case of poly(1,3-dioxepane). As is evident from Figure 8, the COCOC sequences have the *gauche*—*gauche* conformation. This situation is just the same as that for POM. Accordingly, this

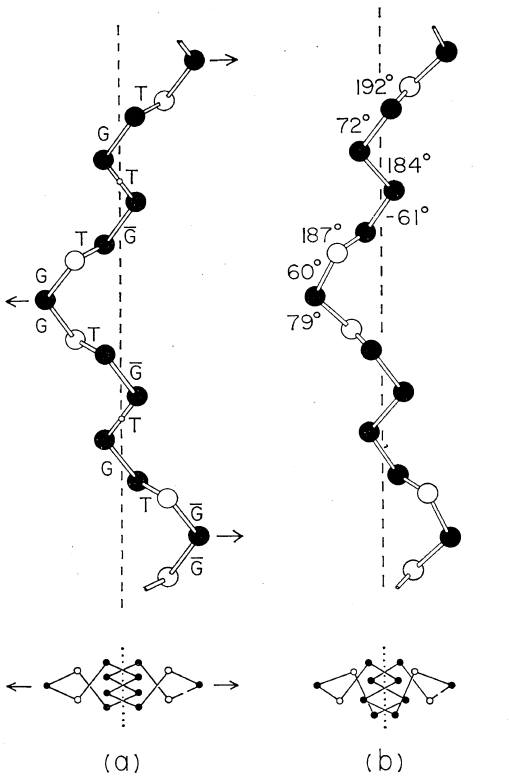

Figure 8. Molecular structure of poly(1,3-dioxepane) with its symmetry elements: (a) model I and (b) final result.

molecular conformation may be considered to be stable from the electrostatic point of view.

The regularity of the bond scission of cyclic formals in cationic polymerization was pointed out by many authors.[9,11,13] In the case of poly(1,3-dioxolane), Okada, Yamashita, and Ishii reported that the bond scission occurs exclusively at bond I, not at II, and confirmed this mechanism from the result of the acid-catalyzed hydrolysis of poly(1,3-dioxolane) and 1,3-dioxolane—styrene copolymer.[9] The regularity of poly(1,3-dioxepane) was supported by Plesch and Westermann from the NMR spectra and from the fact that the solution after depolymerization contains no organic constituents other than monomer and solvent.[11] The present result shows directly that the molecular chain of poly(1,3-dioxepane) consists of a regular sequence of [—OCH_2O—$(CH_2)_4$—]. Accordingly, it was confirmed that the bond scission of 1,3-

dioxepane ring occurs exclusively at the same type of bond (I or II), and never at random.

Acknowledgement. The authors wish to thank Professor Yuya Yamashita of Nagoya University for his valuable suggestion and advice.

REFERENCES

1. For example, H. Tadokoro, *Macromol. Reviews*, **1**, 119 (1967), and the references therein.
2. T. Uchida and H. Tadokoro, *J. Polym. Sci., Part A-2*, **5**, 63 (1967).
3. H. Tadokoro, Y. Takahashi, Y. Chatani, and H. Kakida, *Makromol. Chem.*, **109**, 96 (1967).
4. S. Kobayashi, H. Tadokoro, and Y. Chatani, *ibid.*, **112**, 225 (1968).
5. D. Makino, M. Kobayashi, and H. Tadokoro, *J. Chem. Phys.*, **51**, 3901 (1969).
6. C. W. Bunn, *Nature*, **161**, 929 (1948).
7. H. Sakakihara, Y. Takahashi, and H. Tadokoro, to be published.
8. J. W. Hill and W. H. Carothers, *J. Amer. Chem. Soc.*, **57**, 925 (1935).
9. M. Okada, Y. Yamashita, and Y. Ishii, *Makromol. Chem.*, **80**, 196 (1964).
10. Y. Yamashita, M. Okada, K. Suyama, and H. Kasahara, *ibid.*, **114**, 146 (1968).
11. P. H. Plesch and P. H. Westermann, *Polymer, ibid.*, **10**, 105 (1969).
12. S. Sasaki, Y. Takahashi, and H. Tadokoro, *J. Polym. Sci., Part A-2*, in press.
13. E. F. Oleinik and N. S. Yenikolopyan, *Vysokomol. Soedin., Ser. A*, **9**, 2609 (1967); *Polym. Sci. U.S.S.R.*, **9**, 2951 (1967).
14. S. Arnott and A. J. Wonacott, *Polymer.*, **7**, 157 (1966).
15. Y. Takahashi, T. Satō, H. Tadokoro, and Y. Tanaka, *J. Polym. Sci., Part A-2*, in press.
16. H. Tadokoro, Y. Chatani, T. Yoshihara, S. Tahara, and S. Murahashi, *Makromol. Chem.*, **73**, 109 (1964).
17. Y. Takahashi, H. Tadokoro, and Y. Chatani, *J. Macromol. Sci.*, **B2**, 361 (1968).
18. M. Yokoyama and H. Tadokoro, to be published.
19. H. Tadokoro, M. Kobayashi, Y. Kawaguchi, A. Kobayashi, and S. Murahashi, *J. Chem. Phys.*, **38**, 703 (1963).
20. H. Tadokoro, M. Kobayashi, K. Mori, and R. Chûjô, *Repts. Progr. Polym. Phys. Japan*, **8**, 45 (1965).